

RESEARCH ARTICLE

miR-222 exerts negative regulation on insulin signaling pathway in 3T3-L1 adipocytes

Pere Bibiloni^{1,2,3}  | Catalina A. Pomar^{1,2,3}  | Andreu Palou^{1,2,3}  |
 Juana Sánchez^{1,2,3}  | Francisca Serra^{1,2,3} 

¹Laboratory of Molecular Biology, Nutrition and Biotechnology (Nutrigenomics, Biomarkers and Risk Evaluation), University of the Balearic Islands, Palma, Spain

²Instituto de Investigación Sanitaria Illes Balears, IDISBa, Palma, Spain

³CIBER Fisiopatología de la Obesidad y Nutrición (CIBEROBN), Instituto de Salud Carlos III (ISCIII), Madrid, Spain

Correspondence

Juana Sánchez, Laboratory of Molecular Biology, Nutrition and Biotechnology (Nutrigenomics, Biomarkers and Risk Evaluation), Edificio Mateu Orfila, Carretera de Valldemossa Km 7.5, 07122 Palma de Mallorca, Spain.
 Email: joana.sanchez@uib.es

Funding information

Instituto de Salud Carlos III, Grant/Award Number: PI17/01614; Centro de Investigación Biomédica en Red Fisiopatología de la Obesidad y Nutrición (CIBEROBN); European Union

Abstract

Increased miR-222 levels are associated with metabolic syndrome, insulin resistance, and diabetes. Moreover, rats fed an obesogenic diet during lactation have higher miR-222 content in breast milk and the offspring display greater body fat mass and impaired insulin sensitivity in adulthood. In order to investigate the molecular mechanisms involved and to dissect the specific effects of miR-222 on adipocytes, transfection with a mimic or an inhibitor of miR-222 has been conducted on 3T3-L1 preadipocytes. 3T3-L1 cells were transfected with either a mimic or an inhibitor of miR-222 and collected after 2 days (preadipocytes) or 8 days (mature adipocytes) for transcriptomic analysis. Results showed a relevant impact on pathways associated with insulin signaling, lipid metabolism and adipogenesis. Outcomes in key genes and proteins were further analyzed with quantitative reverse transcription polymerase chain reaction and Western Blotting, respectively, which displayed a general inhibition in important effectors of the identified routes under miR-222 mimic treatment in preadipocytes. Although to a lesser extent, this overall signature was maintained in differentiated adipocytes. Altogether, miR-222 exerts a direct effect in metabolic pathways of 3T3-L1 adipocytes that are relevant to adipocyte function, limiting adipogenesis and insulin signaling pathways, offering a mechanistic explanation for its reported association with metabolic diseases.

Abbreviations: ACTB, beta actin; *Akt2*, AKT protein kinase B; *Cd36*, cluster of differentiation 36; *Cdkn1b*, cyclin-dependent kinase inhibitor 1B; C-inh, negative control of inhibitor; C-mim, negative control of mimic; *Cpt1b*, carnitine palmitoyltransferase 1B; DM, differentiation medium; *Fasn*, fatty acid synthase; FBS, fetal bovine serum; *Gdi*, guanosine diphosphate dissociation inhibitor 1; *Igf1*, insulin-like growth factor 1; *Igf1r*, insulin-like growth factor 1 receptor; *Igf2bp2*, insulin-like growth factor 2 mRNA-binding protein 2; *inh222*, inhibitor of miR-222; *Insig1*, insulin-induced gene 1 protein; *Insr*, INSR, insulin receptor; *IR*, insulin resistance; *Irs1*, insulin receptor substrate 1; *LiPe*, hormone-sensitive lipase; *Lpl*, lipoprotein lipase; *mim222*, mimic of miR-222; mRNA, messenger RNA; miRNA, microRNA; NT-Control, non-transfected control; *Pi3kr1*, phosphatidylinositol 3-kinase regulatory subunit alpha; PM, preadipocyte medium; *Pparγ*, peroxisome proliferator-activated receptor gamma; *Prkaa1*, 5'-AMP-activated protein kinase catalytic subunit alpha-1; *Pten*, PTEN phosphatase and tensin homolog; *Slc2a4*, glucose transporter type 4; *Srebf1*, sterol regulatory element-binding protein.

Pere Bibiloni and Catalina A. Pomar contributed equally to this study.

This is an open access article under the terms of the [Creative Commons Attribution-NonCommercial-NoDerivs](https://creativecommons.org/licenses/by-nc-nd/4.0/) License, which permits use and distribution in any medium, provided the original work is properly cited, the use is non-commercial and no modifications or adaptations are made.

© 2022 The Authors. *BioFactors* published by Wiley Periodicals LLC on behalf of International Union of Biochemistry and Molecular Biology.

KEYWORDS

adipocytes, adipogenesis, insulin resistance, insulin signaling pathway, miR-222

1 | INTRODUCTION

MicroRNAs (miRNAs) are noncoding RNA averaging a length of approximately 22 nucleotides that participate in the posttranscriptional regulation of gene expression. Mainly, miRNAs silence messenger RNA (mRNA) of target genes.¹ Aberrant expression of these molecules can lead to cell malfunction and, ultimately, to disease.^{2,3} Obesity and metabolic diseases have been linked to dysregulated miRNA expression patterns^{4,5} and miR-222 may have a specific role in this context.

Various animal studies support this association. A diet-induced obese mouse model shows increased miR-222 expression in adipose tissue.⁶ Also, rats with spontaneous type 2 diabetes (T2D) present higher miR-222 levels specifically in adipose tissue, whereas no effect is observed in other insulin-target tissues.⁷ Related outcomes have been observed in human studies. Circulating miR-222 levels are significantly upregulated in adults with morbid obesity⁵ and a sixfold raise is observed in children with obesity.⁸ Interestingly, elevated circulating miR-222 levels are reported in T2D patients, either with overweight or obesity, whereas individuals with obesity and normal glucose tolerance do not exhibit this alteration.⁹ In addition, metformin, an insulin sensitizer drug used to treat T2D, decreases the increment of miR-222.⁹ Altogether, these results suggest that, within the broad metabolic disease scenario, miR-222 is particularly involved in repressing the insulin signaling pathway in white adipose tissue and may have a role in the development of insulin resistance (IR).⁴ As it has been previously stated, it “shows arguably the greatest promise as a clinical biomarker of metabolic disease.”⁴

Breast milk is a relevant source of miRNAs.¹⁰ Several studies have shown that maternal body weight or maternal diet can disturb the levels of particular miRNAs in this fluid.^{11–14} It is well-known that lactation is a crucial period to exert long-term effects on the offspring, a concept referred as metabolic programming.^{15,16} Additionally, evidence suggests that milk can act as an exosomal miRNA transmitter, which would be incorporated by breastfed offspring and trigger epigenetic modifications.^{17,18} In a recent study, we have shown that cafeteria diet (rich in carbohydrates and lipids) during lactation raises miR-222 levels in milk (among other miRNAs).¹³ Descendants of the dams display a thin-outside-fat-inside phenotype in their adulthood: greater fat accumulation despite no body weight gain and altered insulin signaling

(impaired response to an oral glucose tolerance test).¹⁹ They also present an impairment in the fed/fasting response postweaning²⁰ and an altered diet-induced thermogenesis in their adulthood,²¹ showing a general metabolic inflexibility in the adipose tissue. Results support that raised miR-222 levels in breast milk could be in part responsible for the long-term changes observed in offspring and metabolic programming effects due to miRNAs variations are suggested.¹³

In order to investigate the molecular mechanisms involved and to dissect the specific effects of miR-222 on adipocytes, we have transfected 3T3-L1 preadipocytes with either a mimic or an inhibitor of miR-222 aiming to determine whether its overexpression can lead to the observed long-term effects on insulin signaling and adipogenesis pathways.

2 | EXPERIMENTAL PROCEDURES

2.1 | Experimental design at a glance

The workflow is schematized in Figure 1. Two days upon confluence completion (day 0), 3T3-L1 preadipocytes were transfected with either a miR-222 mimic (mim222), a miR-222 inhibitor (inh222), or their respective negative controls (C-mim or C-inh). Non-transfected cells were cultured in parallel as a control group (NT-Control). Half of the wells were collected at day 2 (preadipocyte condition) and the remainder at day 8 after completing their differentiation to mature adipocytes. Total lipid content was analyzed on mature adipocytes from groups mim222, C-mim, and NT-Control by oil red O staining to assess the impact of the treatments in lipid storage capacity. All the other determinations were performed with cells from both stages (preadipocytes and mature adipocytes). miR-222 levels were determined by quantitative reverse transcription polymerase chain reaction (RT-qPCR) in cells from all experimental groups in order to assess whether transfection was successfully performed. Transcriptomic analysis (microarray technique) was performed in a subset of samples and included cells from mim222, C-mim, and NT-Control treatments. Bioinformatic analysis of signaling routes was conducted to determine the global effect of the transfection. Next, the expression of selected genes related to the relevant identified pathways was determined by RT-qPCR to confirm the effects observed. In this analysis, samples from all experimental

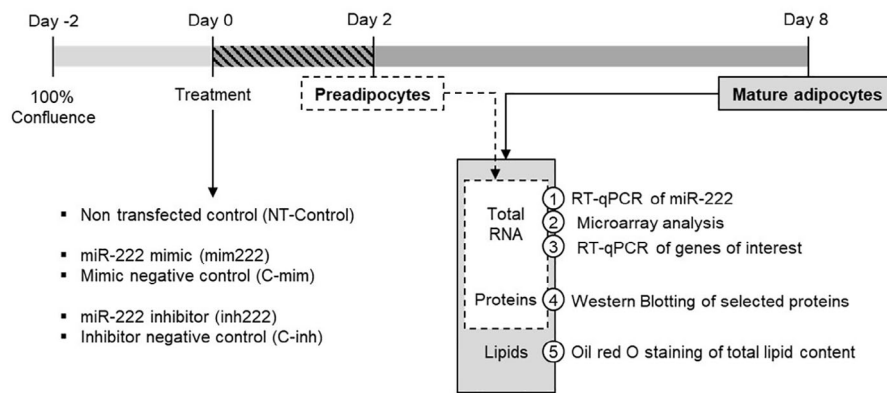


FIGURE 1 Scheme of the experimental design applied to murine 3T3 L1 fibroblasts in culture and transfected either with a miR-222 mimic (mim222) or a miR-222 inhibitor (inh222) at confluence (day 0). Half of cells were collected at day 2 (preadipocyte status) and the rest after reaching the state of mature adipocytes (day 8). Gene and protein expression analyses were performed. Respective controls of transfections were used (C-mim and C-inh) as well as non-transfected control cells (NT-Controls) to check performance of transfection and impact on cell growth.

treatments were included. Finally, in order to assess whether changes in mRNA levels would have a repercussion on cell functionality, expression of proteins of interest was analyzed by Western Blotting. To this purpose and considering previous results, studies were performed on mim222, C-mim, and NT-Control cells.

2.2 | Cell culture and transfection

Murine 3T3-L1 fibroblasts were purchased from ZenBio (Durham, NC, USA). Cells were cultured in preadipocyte medium (PM-1-L1) at 37°C in 10% CO₂. At 80% of confluence, cells were subcultured and allowed to reach 100% confluence (day -2). After 48 h (day 0), cell specialization was induced by differentiation medium (DM-2-L1), containing 5 µg/ml insulin, 0.5 mmol/l 3-isobutyl-1-methyl-xantine, 0.5 µmol/l dexamethasone, 100 U/ml penicillin, 100 µg/ml streptomycin and 10% fetal bovine serum (FBS) in Dulbecco's modified Eagle's medium-high glucose (DMEM). Then, culture conditions were changed to 8% CO₂, maintaining 37°C and saturated humidity. In addition, at day 0, transfection was carried out using lipofectamine RNAiMAX Reagent (Life Technologies, Madrid, Spain) as indicated by manufacturer's instructions. Cells were transfected with 50 nM miR-222 mimic (mim222) (Assay ID MC11376), 50 nM miR-222 inhibitor (inh222) (Assay ID MH11376), 50 nM mimic negative control (C-mim), or 50 nM inhibitor negative control (C-inh). All RNA transfection reagents were purchased from Life Technologies. In parallel, we followed a subset of cells that were not transfected at all (NT-Control). The performance of miRNA transfection was validated by using two positive controls of transfection: one for the

mimic effect (miR-1) and another for the inhibitor (anti-mir let-7c) (Life Technologies), as previously published.²² In order to minimize treatment-related heterogeneity, cells were cultured in several plates, each one containing samples from the different treatments. Moreover, results are from three independent cultures performed at different times.

At day 2, half of the plates were collected constituting the preadipocytes group of cells. For the remaining plates, culture medium was changed to maintenance medium, containing DMEM with 5 µg/ml insulin, 100 U/ml penicillin, 100 µg/ml streptomycin, and 10% FBS. Culture medium was replaced every 2 days. At day 8, remaining cells were collected as they were fully differentiated into mature adipocytes, which was assessed by morphological changes and lipid droplets accumulation.

2.3 | Oil red O staining

Total lipid content was assessed at day 8 in cells from mim222, C-mim, and NT-Control treatments by staining cells with oil red O prior its fixation with formalin. First, cells were washed with phosphate buffered saline (PBS) and fixed with 10% formaldehyde in PBS during 1 h at room temperature. Next, two washes with water and one wash with 60% isopropanol were performed. After that, staining was done incubating for 1 h the mature adipocytes with oil red O (0.35 g oil red O in 100 ml isopropanol diluted with double distilled water [40:60] and filtrated). Finally, unbound dye was removed with a final wash of water, stained cells were visualized by light microscopy and photographs were taken. In order to quantify the fat accumulation, the stain was eluted from

cells with isopropanol and the absorbance at 500 nm was measured.

2.4 | Total RNA extraction

Total RNA was isolated from collected preadipocytes and mature adipocytes according to Tri Reagent protocol guidelines (Sigma Aldrich Química SA, Madrid, Spain). RNA from samples was quantified on Nanodrop ND-1000 spectrophotometer (NanoDrop Technologies Inc., Wilmington, DE, USA). Optimal A260/A280 and A260/230 ratios were assessed to verify its integrity.

2.5 | miR-222 quantification

In order to determine the specific levels of miR-222, first a universal reverse transcription step was carried out using miRCURY LNA RT Kit, according to manufacturer's guidelines (QIAGEN, Madrid, Spain). Then, 10 ng of total RNA were used to synthesize complementary DNA. The reactions were done in an Applied Biosystems 2720 Thermal Cycler (Applied Biosystems, Madrid, Spain) at 42°C for 60 min, 95°C for 5 min and a final holding step at 4°C. From 1/30 dilution of the product, miR-222 was specifically amplified utilizing the miRCURY LNA SYBR Green PCR Kit (QIAGEN) following the protocol instructions. An Applied Biosystems StepOnePlus Real-Time PCR System (Applied Biosystems) was used to perform the following schedule: 95°C for 2 min and 40 cycles of 95°C for 10 s and 56°C for 60 s, followed by a melting curve analysis. Finally, StepOne Software v2.3 permitted to obtain the threshold cycle (Ct) values that were subsequently used to determine the relative levels of miR-222 by the $2^{-\Delta\Delta Ct}$ method with guanosine diphosphate dissociation inhibitor 1 (*Gdi*) as the reference gene.

2.6 | Microarray processing and data analysis

RNA extracted from both preadipocytes and mature adipocytes from mim222, C-mim, and NT-Control treatments ($n = 4$ in each group) was processed for microarray analysis. Procedure was carried out by "Servicio de Genómica y Genética Traslacional" from the "Centro de Investigación Príncipe Felipe" (Valencia, Spain). Quality of the samples was assured with an RNA integrity number superior to 9. This control was performed on Agilent 2100 Bioanalyzer with RNA 6000 Nano chips (Agilent Technologies, Barcelona, Spain). Microarray

processing was done using Mouse GE $8 \times 60K$ Microarray according to manufacturer's protocol (Agilent Technologies). Raw data background was corrected following the Agilent methodology continuing with its standardization by quantile normalization. Differences in expression were calculated with moderate *t*-statistic of the Limma package and adjusting the *p*-values using Benjamini-Hochberg method. In addition, an analysis of signaling routes with hiPathia was performed.²³ Contrast between two treatments was done with Limma to check whether the route had been activated or inhibited. Fold change of the effect was calculated and expressed as binary logarithm (log FC). Contrasts studied were mim222 versus C-mim (to test the effect of the miR-222) and NT-Control versus C-mim (to assess bias effects from the transfection procedure) from both preadipocytes and mature adipocytes.

2.7 | Quantitative reverse transcription polymerase chain reaction

An amount of 0.2 μ g of total RNA isolated from cultured cells was used to perform reverse transcription with the iScript cDNA synthesis kit (Bio-Rad Laboratories, S.A., Madrid, Spain), according to protocol's instructions. Then, 1/10 dilution of the cDNA product was used to perform qPCR with forward and reverse primers (5 μ M each) (Sigma Aldrich Química SA, Madrid, Spain) and Power SYBER Green PCR Master Mix (Life Technologies). The procedure was carried out using the Applied Biosystems StepOnePlus Real-Time PCR Systems (Applied Biosystems). The cycling conditions were an initial Taq polymerase activation cycle of 95°C for 10 min and 40 two-temperature cycles of 95°C for 15 s and 60°C for 1 min each. StepOne Software v2.3 was used in order to calculate the threshold cycle (Ct) values. $2^{-\Delta\Delta Ct}$ method was utilized to standardize the expression using Ct of the housekeeping gene. *Gdi* presented a uniform expression between different groups, therefore was selected as the reference gene. Finally, mRNA levels of mim222 or inh222 treatments were expressed as percentage of the negative control, C-mim or C-inh, respectively.

2.8 | Western Blotting

Protein levels of insulin receptor (INSR), phosphatase and tensin homolog (PTEN), and protein kinase B (AKT) were determined by Western Blotting. Beta actin (ACTB) was also determined to be used as transfer and loading control. To perform total protein extraction, cell wells were scrapped in 500 μ l of RIPA buffer containing Halt

Protease and Phosphatase Inhibitor Cocktail (Thermo Fisher, Rockford, IL, USA). Next, total proteins were quantified using the bicinchoninic acid assay following the manufacturer's instructions. Then, 20 μ g of RIPA protein extracts were loaded in a 4–20% SDS-PAGE (Criterion TGX, Bio-Rad Laboratories). After separation, proteins were transferred to a nitrocellulose membrane (Bio-Rad Laboratories) continuing with the blocking procedure. Membranes were incubated with the primary antibodies (anti-INSR, #3025 S; anti-AKT, #9272; anti-PTEN, #14642; anti-ACTB, #3700; Cell Signaling Technology, Danvers, MA, USA) preceding incubation with the corresponding infrared-dyed secondary anti-IgG antibodies (anti-Rabbit IgG, 926-32211; anti-Mouse IgG, 926-68020; Li-COR Biosciences, Lincoln, NE, USA). Finally, membranes were scanned in Odyssey Infrared Imaging System (LI-COR Biosciences) and bands obtained were quantified using the software Odyssey v3.0 (LI-COR Biosciences).

2.9 | Statistical analysis

Statistical analysis of microarray data is detailed in the respective section. With respect to RT-qPCR and Western Blotting experiments, values are presented as the mean \pm SEM with $n = 4$ –10 samples in each treatment. Single comparisons were assessed by Mann–Whitney U test as number of samples per group was inferior or equal to 10. p -Value < 0.05 was considered as statistically significant. SPSS Statistics 21.0 (SPSS, Chicago, IL, USA) software was used to compute statistics analyses.

3 | RESULTS

3.1 | Transfection performance and adipocyte differentiation assessment

In NT-control cells, native miR-222 levels showed a downward tendency (43% decline, $p = 0.053$) in mature adipocytes compared to preadipocytes (Figure 2A), which would indicate that miR-222 expression is diminished during adipocyte differentiation.

Regarding cells transfected with the mimic for miR-222 (mim222 treatment), they exhibited much greater levels of miR-222 compared to the corresponding controls (C-mim) in both preadipocytes (x1381) and mature adipocytes (x435) (Figure 2B). Remarkably, the impact observed on mature adipocytes was lower than at the earlier stage, in accordance with the decrease observed with endogenous miR-222 in non-transfected cells (NT-control treatment). As expected, cells transfected with the

inhibitor (inh222 treatment) displayed diminished levels of miR-222 in comparison with controls (C-inh), for both preadipocytes (90%) and mature adipocytes (43%) (Figure 2C), even though at day 8, this reduction was more discreet and did not reach statistical significance.

These initial outcomes prove that transfections performed were successful and confirm this *in vitro* model as a valid approach to study the effects of miR-222 at the molecular level. Moreover, they showed that changes induced in miR-222 levels at early stages, either by the mimic or the inhibitor, could remain throughout the differentiation process and still be manifested after adipocyte commitment, although at a lower extent.

In addition, oil red O staining was performed to assess lipid droplet accumulation on mature adipocytes from mim222, C-mim, and NT-Control treatments ($n = 7$ –10) (Figure 2D). No differences were seen in the lipid content comparing NT-Control and C-mim (Figure 2E), suggesting that the transfection procedure did not disturb the physiological process under cell specialization. Given mim222 versus C-mim contrast, no significant differences were observed neither visually nor quantitatively in lipid content. A further impact on the profile of lipid species was not studied but should not be discarded as a potential effect of mim222 transfection.

3.2 | Untargeted gene expression analysis on the effects of miR-222 transfection

A microarray analysis was performed with a subset of 24 samples from both preadipocytes and mature adipocytes, including mim222, C-mim, and NT-Control experimental treatments (four samples per group). Differential expression analysis of microarray results showed that the transfection with miR-222 altered the expression of 2045 genes in preadipocytes (950 genes underexpressed and 1095 overexpressed compared to C-mim) while in mature adipocytes this number was reduced to 1160 (544 genes repressed and 616 genes stimulated).

We focused on a holistic approach to check for differences in signaling pathways, using hiPathia method.²³ Results from hiPathia analysis of signaling routes showed that, for the contrast between controls (NT-Control vs. C-mim), 14 pathways were altered in preadipocytes, while none was affected in mature adipocytes. These pathways were excluded in the following analyses, since it was assumed that these changes were not specifically caused by mimic treatment. Comparing mim222 and C-mim, in preadipocytes 66 routes were significantly downregulated while 74 were upregulated (Table S1A, Supporting Information). Among them, 17 were selected for their

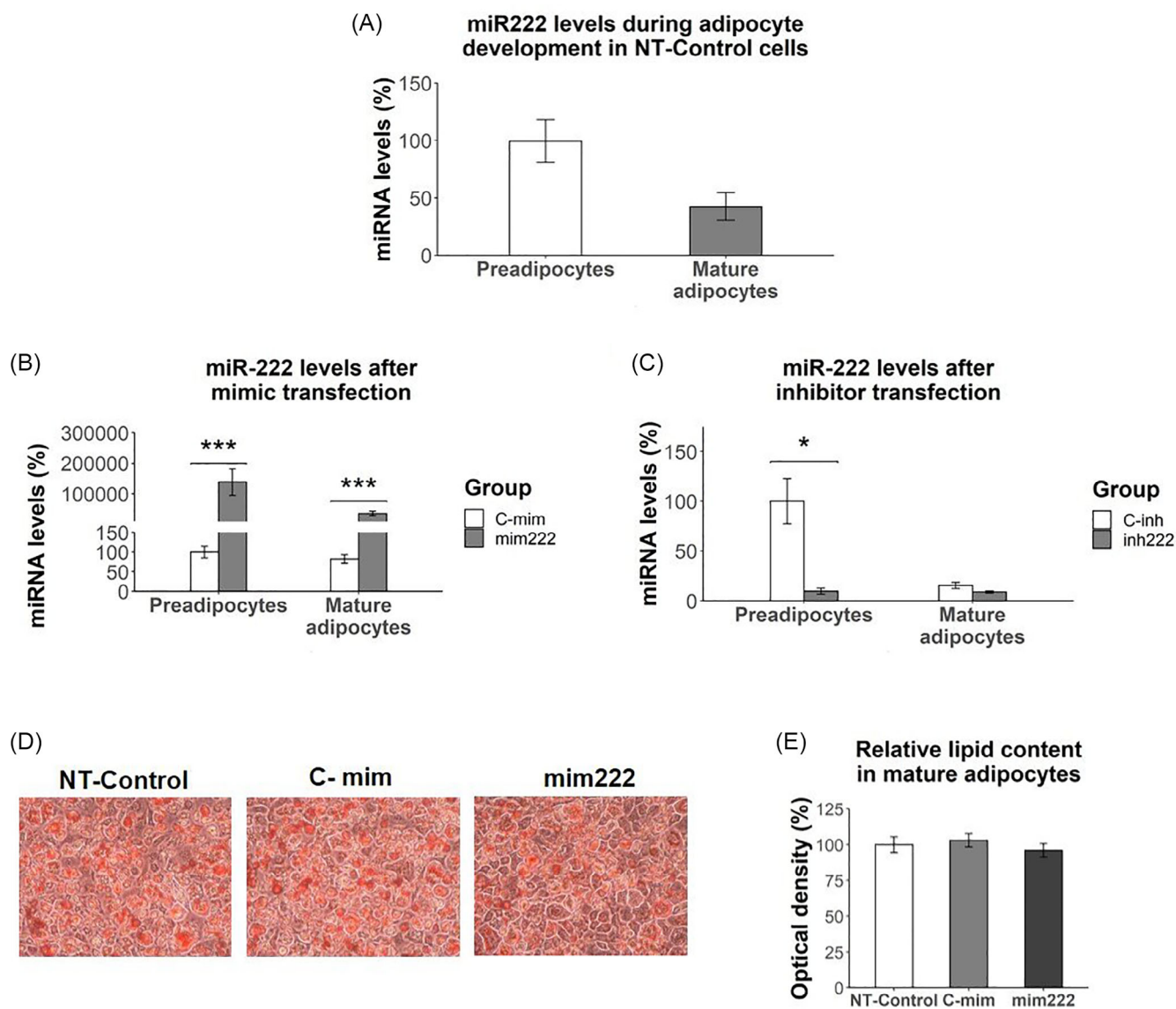


FIGURE 2 Evaluation of transfection performance and adipocyte differentiation. (A) Endogenous miR-222 levels in NT-Control cells from both cell stages. (B) Overexpression of miR-222 induced by transfection with the miR-222 mimic (mim222) and the respective control treatment (C-mim) in both cell stages. Expression of C-mim from preadipocytes was considered the value for reference (100%). (C) Repression of miR-222 induced by transfection with the miR-222 inhibitor (inh222) and the respective control treatment (C-inh) in both cell stages. Expression of C-inh from preadipocytes was considered the value for reference (100%). miRNA levels were measured by quantitative reverse transcription polymerase chain reaction (RT-qPCR), calculated with $2^{-\Delta\Delta Ct}$ method and expressed as percentage of the respective reference group. Data are mean \pm SEM. Statistics from Mann–Whitney U test: * $p < 0.05$; *** $p < 0.001$. (D) Representative microphotographs at 10 \times of oil red O stained mature adipocytes from the different treatments. (E) Semiquantitative levels of lipid content from oil red O staining in mature adipocytes.

biological plausibility, as they are related to the insulin signaling pathway, the adipogenesis process, the endocrine function of the adipose tissue or the energy homeostasis (Table 1A). In mature adipocytes, for the same contrast, 49 routes were repressed and 49 pathways were overexpressed (Table S1B, Supporting Information), indicating a more discreet but still significant long-lasting effect of the treatment. Taking into account their potential impact on the normal function of adipocytes, seven of them were of particular interest (Table 1B), showing a

reduction of the impact of the mim222 after cell differentiation. Interestingly, three routes, related to insulin signaling pathway, energy metabolism and adipogenesis were significantly inhibited under the mim222 effect in both cell differentiation stages: *Insulin signaling pathway: D-glucose*, *Central carbon metabolism in cancer: Pten* and *PPAR signaling pathway: Aqp7*.

Altogether, these results suggest that transfection with a miR-222 mimic at the beginning of the adipocyte differentiation impacts a considerable number of mRNA

TABLE 1 Selection of signaling routes significantly altered in mim222 treatment in contrast with C-mim in preadipocytes (A) or in mature adipocytes (B) according to hiPathia analysis. The logarithm of the fold change (log FC) indicates whether the pathway is inhibited (negative value, at the top) or induced (positive value, at the bottom). Routes are listed by increasing adjusted *p*-value (Adj.*p.val*). Routes in bold are significantly altered in mim222 treatment in both cell stages

(A) Signaling routes significantly altered in preadipocytes			
ID	Name	log FC	Adj.<i>p.val</i>
P-mmu04930-3	Type II diabetes mellitus: Slc2a4	-0.1082	0.0001
P-mmu03320-53	PPAR signaling pathway: Adipoq	-0.1003	0.0011
P-mmu05230-100	Central carbon metabolism in cancer: Pten	-0.0285	0.0011
P-mmu04910-17	Insulin signaling pathway: D-Glucose	-0.0232	0.0011
P-mmu03320-7	PPAR signaling pathway: Aqp7	-0.0448	0.0046
P-mmu03320-31	PPAR signaling pathway: Cd36	-0.0577	0.0207
P-mmu03320-40	PPAR signaling pathway: Fabp4	-0.0695	0.0267
P-mmu04152-35	AMPK signaling pathway: Pfkfb3	-0.0153	0.0289
P-mmu04152-87	AMPK signaling pathway: Cd36	-0.0267	0.0328
P-mmu03320-8	PPAR signaling pathway: Gk2	-0.0272	0.0409
P-mmu04920-43	Adipocytokine signaling pathway: Fatty acid	-0.0583	0.0457
P-mmu04920-10	Adipocytokine signaling pathway: Pck1	0.0206	0.0011
P-mmu04152-52	AMPK signaling pathway: Pck1	0.0108	0.0139
P-mmu04151-100	PI3K-Akt signaling pathway: Prkca	0.0067	0.0287
P-mmu04151-4	PI3K-Akt signaling pathway: 105244208	0.0051	0.0294
P-mmu04920-9	Adipocytokine signaling pathway: G6pc	0.0125	0.0364
P-mmu04920-1	Adipocytokine signaling pathway: N-Acylsphingosine	0.0212	0.0367
(B) Signaling routes significantly altered in mature adipocytes			
ID	Name	log FC	Adj.<i>p.val</i>
P-mmu05230-100	Central carbon metabolism in cancer: Pten	-0.0249	0.0054
P-mmu04152-68	AMPK signaling pathway: Ppargc1a	-0.0116	0.0095
P-mmu04152-54	AMPK signaling pathway: Slc2a4	-0.0155	0.0100
P-mmu03320-36	PPAR signaling pathway: Slc27a1	-0.0432	0.0190
P-mmu04910-17	Insulin signaling pathway: D-Glucose	-0.0170	0.0215
P-mmu04922-51	Glucagon signaling pathway: G6pc	-0.0174	0.0229
P-mmu03320-7	PPAR signaling pathway: Aqp7	-0.0366	0.0290

targets and that, to a lower extent, these effects remain until final steps of cell maturation. Taking this into consideration, further analyses of genes of interest involved in the outlined routes were performed.

3.3 | Targeted gene expression analysis on the effects of miR-222 transfection

RT-qPCR analyses were carried out in order to determine the impact of the transfection on the expression of selected genes related to the above featured routes. Samples from all experimental groups and both cell stages

were included. Overall, there were not significant differences between NT-Control and C-mim or C-inh groups (data not shown), suggesting that the transfection process itself did not have a relevant impact on gene expression.

Regarding the effect of the mimic (mim222 vs. C-mim), results from preadipocytes showed a general inhibitory impact on most genes studied (Figure 3A). Genes involved in insulin signaling pathway (Insulin receptor [*Insr*]; INSR substrate 1 [*Irs1*] and phosphatidylinositol 3-kinase regulatory subunit alpha [*Pik3r1*]); on glucose uptake (glucose transporter type 4 [*Slc2a4*]); cholesterol biosynthesis (insulin-induced gene 1 protein [*Insig1*]); fatty acid uptake (lipoprotein lipase [*Lpl*] and cluster of

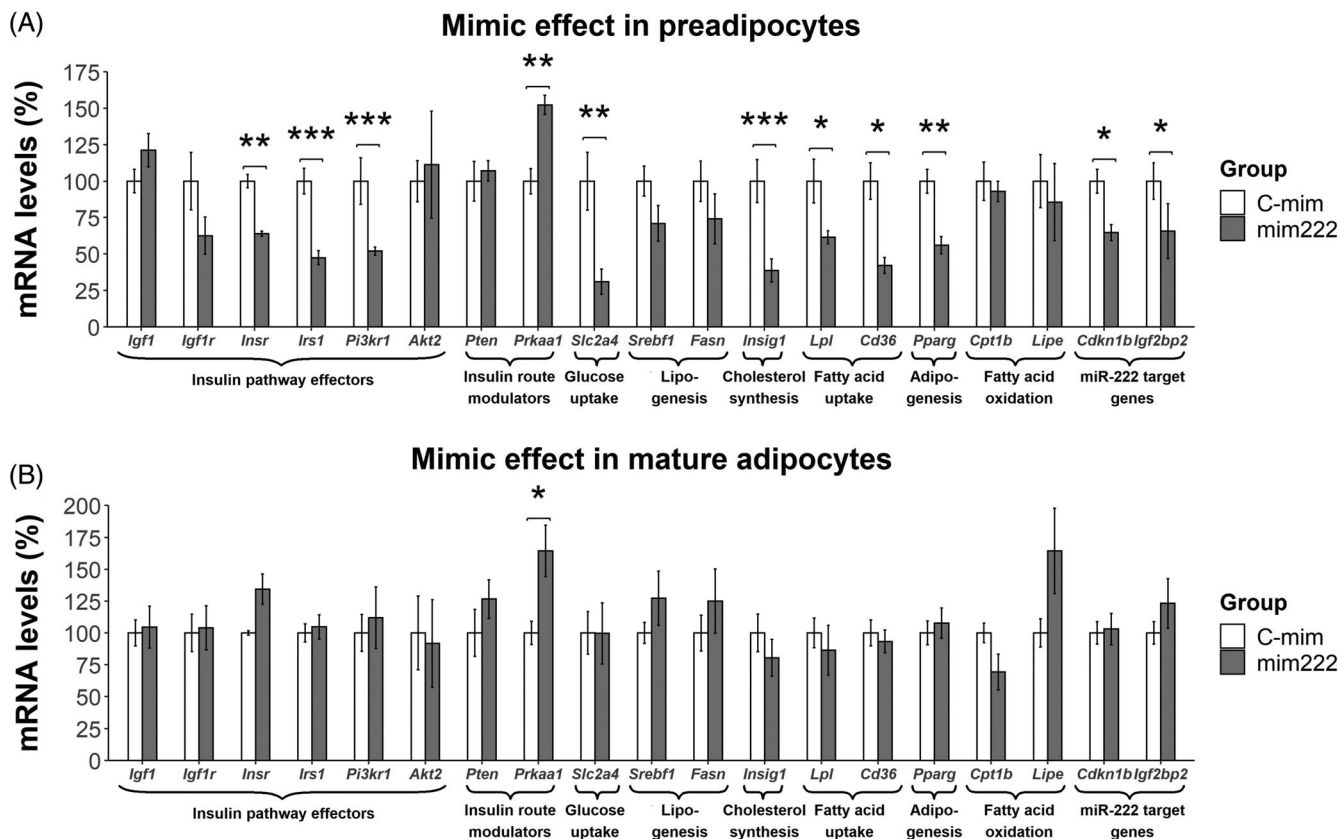


FIGURE 3 mRNA expression of selected genes in 3T3 L1 after transfection with miR-222 mimic (mim222) and the respective control treatment (C-mim) in preadipocytes (A) and in mature adipocytes (B). Gene expression was measured by quantitative reverse transcription polymerase chain reaction (RT-qPCR), calculated with $2^{-\Delta\Delta C_t}$ method and expressed as a percentage of the value of C-mim group. Data are mean \pm SEM. Statistics from Mann-Whitney U test: * $p < 0.05$; ** $p < 0.01$; *** $p < 0.001$.

differentiation 36 [*Cd36*]) and adipogenesis (peroxisome proliferator-activated receptor gamma [*Pparg*]) were repressed (36–69%) due to mim222 transfection. Notably, the only gene overexpressed (52%) under the experimental conditions compared to C-mim was the 5'-AMP-activated protein kinase catalytic subunit alpha-1 (*Prkaa1*), involved in modulating the insulin signaling pathway. Remarkably, the gene cyclin-dependent kinase inhibitor 1B (*Cdkn1b*),²⁴ considered a miR-222 target and the theoretical miR-222 target gene insulin-like growth factor 2 mRNA-binding protein 2 (*Igf2bp2*),²⁵ were both significantly repressed (35 and 34%, respectively). Therefore, the impact seen on the expression of both miR-222 target genes and on the representing genes of the pathways identified as sensible to the action of miR-222, confirms our hypothesis and contributes to validate the results.

Outcomes on gene expression from mature adipocytes displayed a different picture (Figure 3B). The inhibitory effect was lost in all the genes studied. Moreover, a modest tendency to increase mRNA levels was observed in most cases, but without reaching any statistical

significance. Solely *Prkaa1* was maintained overexpressed in the mim222 group compared to C-mim group (1.64-fold).

With respect to the impact observed with the miR-222 inhibitor treatment (inh222 vs. C-inh), results from preadipocytes showed that most of the genes' expression was not altered (Figure 4A). Only three genes related with lipid metabolism (Sterol regulatory element-binding protein [*Srebf1*], *Lpl* and hormone-sensitive lipase [*Lipe*]) were significantly overexpressed in the presence of inh222 in comparison with the respective control (69, 41, and 68%, respectively). In the same way, no general effects were seen in mature adipocytes (Figure 4B). Solely *Cd36* mRNA levels displayed a significant increase of 72% under inh222 conditions compared to C-inh group.

3.4 | Insulin-related protein levels

To verify whether transcriptional changes were also observed at translational level, Western Blot analysis was performed to study the proteins INSR, PTEN, and AKT

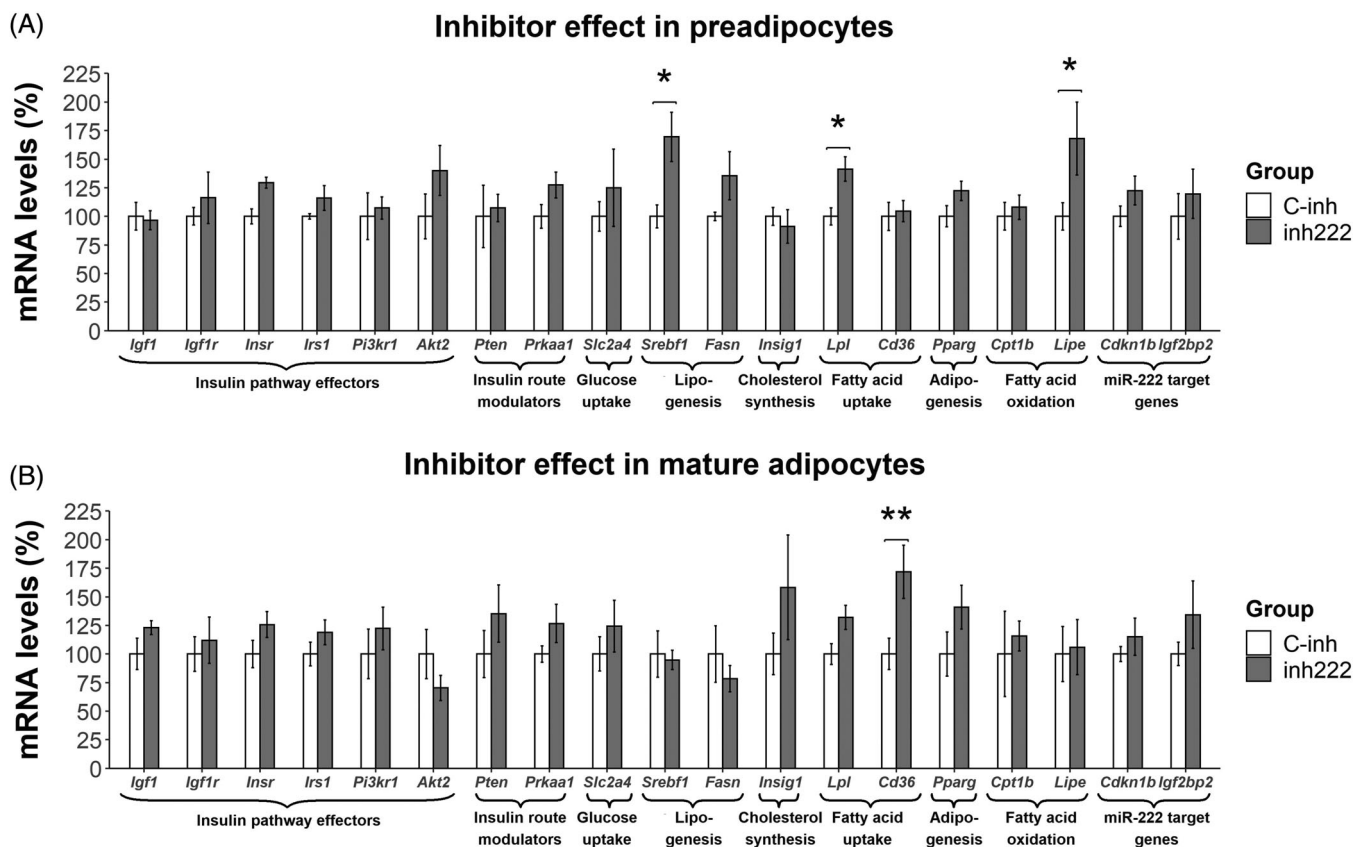


FIGURE 4 mRNA expression of selected genes in 3T3 L1 after transfection with miR-222 inhibitor (inh222) and the respective control treatment (C-inh) in preadipocytes (A) and in mature adipocytes (B). Gene expression was measured by quantitative reverse transcription polymerase chain reaction (RT-qPCR), calculated with $2^{-\Delta\Delta C_t}$ method and expressed as percentage of the value of C-mim group. Data are mean \pm SEM. Statistics from Mann–Whitney *U* test: **p* < 0.05; ***p* < 0.01.

in mim222, C-mim, and NT-Control cells from both differentiation stages. Inhibitor treatments were not included as previous results of changes in gene expression were negligible. NT-Control groups did not exhibit significant differences compared to negative controls, thus denying a bias effect of the transfection process (data not shown).

Outcomes from preadipocytes showed no differences when comparing mim222 with the control (C-mim) treatment (Figure 5A). Nevertheless, in mature adipocytes decreased PTEN and AKT protein levels were observed associated with the mim222 treatment (53 and 37%, respectively) (Figure 5B). Altogether, data suggest that a delayed response from transcription to translation along cell differentiation was taking place.

4 | DISCUSSION

We have previously described that breast milk miR-222 levels are increased in rats fed an obesogenic diet during lactation,¹³ a situation that induces metabolic

programming toward obesity and impaired glucose homeostasis in offspring.¹⁹ We aimed to assess the specific role of miR-222 and to elucidate its molecular effects in adipocytes by transfecting 3T3-L1 cells with miR-222 mimic or inhibitor. Previous results have confirmed that this cell system is sensitive enough to show both the impact of overexpression and blockade of expression of specific miRNAs by transfection.^{22,26,27} Here, we demonstrated that miR-222 levels were modulated due to experimental treatments and that this had a significant repercussion on cell transcriptome. The effects caused by the miRNA inhibitor treatment were more discreet, limited to a few transcripts, a result that agrees with other published works.^{22,26}

During adipocyte commitment, endogenous levels of miR-222 decreased in untransfected cells (NT-Control). This agrees with previous studies, in which miR-222 is downregulated in 3T3-L1 cells during adipogenesis, the process of adipocyte differentiation.²⁸ Conversely, in adipocytes from obese mice its levels are increased.²⁸ This disturbed miRNA expression might affect the functionality of the adipose cell, a situation that was mirrored in

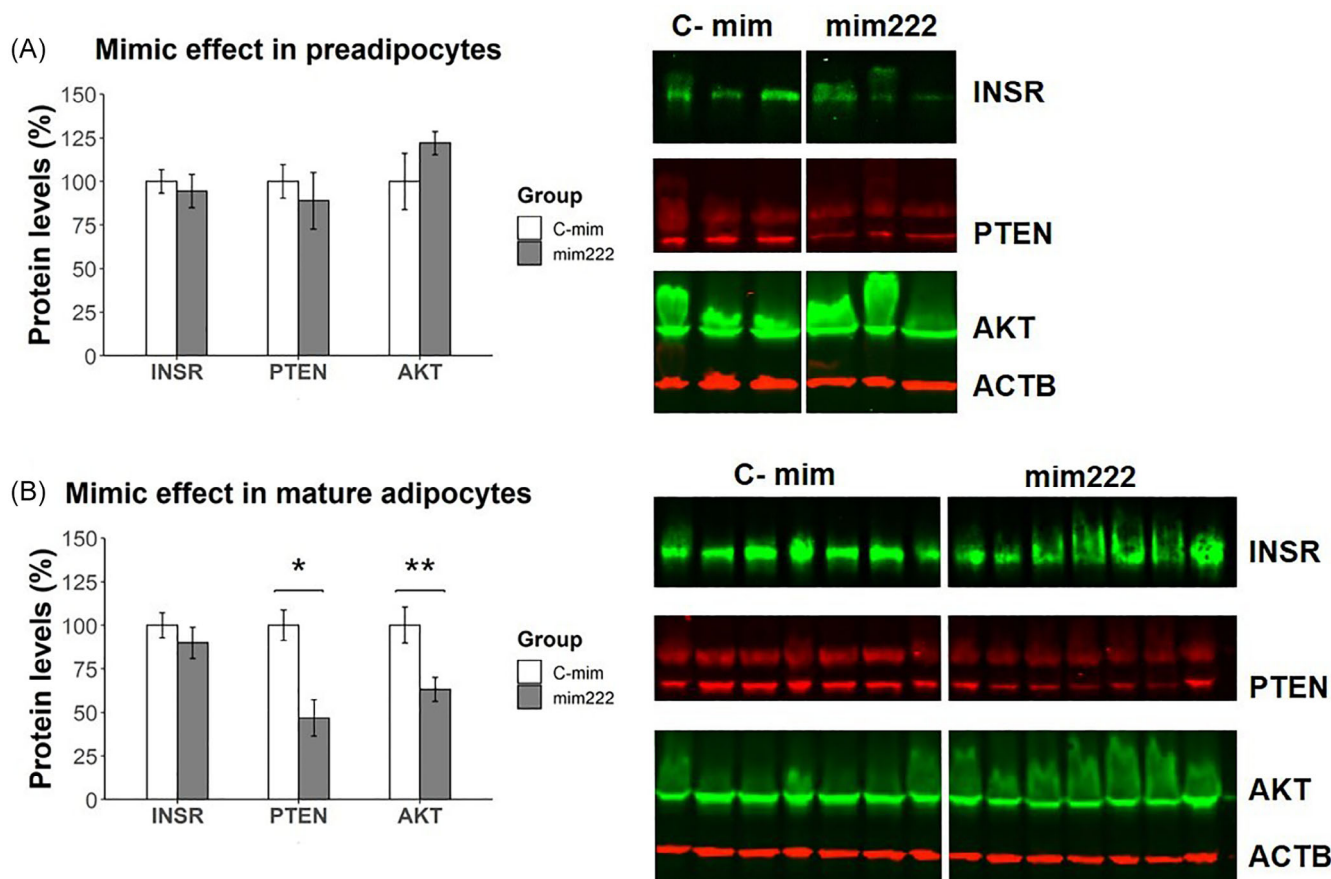


FIGURE 5 Protein levels of INSR, PTEN, and AKT after the treatment with the miR-222 mimic (mim222) and the respective control (C-mim) in preadipocytes (A) and mature adipocytes (B). Representative bands are shown (right panel). Proteins were assessed by Western Blot following labeling with specific fluorescent antibodies. Quantification of individual bands were corrected by ACTB signal and expressed as percentage of the value of C-mim treatment. Data are mean \pm SEM. Statistics from Mann-Whitney *U* test: * $p < 0.05$; ** $p < 0.01$.

this experiment by mim222 treatment. As hypothesized, this overexpression led to changes in gene expression and protein levels that can be linked to the onset of IR and metabolic syndrome, as it will be discussed next grouping these variations by their biological function.

Direct effectors of insulin signaling pathway showed a significant transcriptional inhibition associated with mim222 transfection. Globally, this was seen in the microarray results in both cell stages. From the targeted analyses of *Insr* and *Irs1*, data at preadipocyte stage is higher conclusive at this respect. These results are in agreement with the fact that *Insr* fat-specific knockout (KO) in mice causes marked IR²⁹ and, on the contrary, its overexpression partially improves a diabetic phenotype.³⁰ Regarding *Irs1*, a KO model displays mild IR.³¹ Furthermore, a previous study conducted in a mouse model shows that in liver, increasing miR-222 decreases *Irs1* expression and confirms that this gene is a direct miR-222 target.³² The present work extends these outcomes to adipocytes. Considering the downstream effectors PI3K and AKT, microarray results showed that this

signaling circuit was altered by mim222 transfection. A downward trend was found by RT-qPCR method, particularly at the level of *Pik3r1* mRNA, in mim222 treated preadipocytes. This gene encodes for the p85 α regulatory subunit of PI3K and mutations in this gene have been related with IR in both animals³³ and humans.³⁴ Moreover, decreased *PIK3R1* expression in visceral adipose tissue has been linked to gestational diabetes in humans.³⁵ Concerning AKT, this protein is recognized as essential for correct insulin sensitivity and its activation has been proposed as a strategy to improve IR.³⁶ Despite no differences were observed associated to the influence of the mimic at the level of gene expression, AKT protein synthesis was repressed, particularly in mature adipocytes, which is also a mechanism of action of miRNAs. As a whole, mim222 transfection caused a significant repression of direct effectors of the insulin signaling pathway, which is in turn linked to an IR phenotype.³⁷

In contrast, a potential compensatory mechanism against the implementation of this long lasting IR status seemed to be promoted at the level of the modulators of



the insulin signaling pathway. The signaling route involving *Pten* was found repressed under the mim222 treatment in both cell stages (microarray data). As seen for AKT, the impact of mim222 was not found on the gene expression of *Pten* but on PTEN protein, which was highly reduced in mature adipocytes. Interestingly, mice lacking PTEN in adipose tissue display an improvement in systemic glucose tolerance and insulin sensitivity.³⁸ *Prkaa1*, the coding gene of the AMPK catalytic subunit, which acts like a cellular energy sensor, displayed higher mRNA levels under mim222 treatment in both stages. Contrarily, lower activity of this enzyme is found in adipose tissue in animal models for metabolic syndrome and in humans with IR.³⁹ Altogether, PTEN and *Prkaa1* follow a contrary trend to that expected in an IR scenario, showing cell adaptive responses aiming to cope with insulin dysregulation associated with the stress induced by mim222 transfection.

Checking downstream effectors of insulin signaling pathway on glucose uptake, its key transporter in adipose tissue (GLUT4) was selected.⁴⁰ A signaling route related to T2D and involving GLUT4 was the most inhibited in mim222 preadipocytes and the down-regulation of *Slc2a4*, its coding gene, confirmed this impact. In accordance, specific KO of GLUT4 in adipose tissue leads to a global IR phenotype, affecting main organs such as liver and muscle^{41,42}; and several animal and human studies have shown that GLUT4 expression is selectively diminished in obesity and T2D.⁴³ Hence, mim222 transfection could be linked to impaired insulin tolerance mediated by depressed glucose uptake in insulin-dependent cells.

The expression of genes related to lipid metabolism was also analyzed. In concrete, *Insig1*, which is related to insulin function and lipid synthesis, showed a downregulation under the mim222 treatment in the preadipocyte state. The reduction in *Insig1* levels has been shown to facilitate transcription of lipogenic genes and cholesterol biosynthesis.⁴⁴ In agreement, genetic and dietary mice models of obesity and IR show decreased expression of *Insig1* in white adipose tissue.⁴⁵ These outcomes are also observed in adipocytes from humans with obesity or morbid obesity, and the decrease is even more drastic in subjects with IR.⁴⁵ Thus, mim222 may contribute to IR status by modulating lipid related genes.

Concerning the pathway analysis on cell fatty acid uptake, routes specifically involving *Cd36* appeared downregulated in preadipocytes. This was further confirmed at the level of *Cd36* and *Lpl* expression. Interestingly, the inh222 treatment was efficient to counteract this influence, as *Lpl* was induced in preadipocytes and *Cd36* in mature adipocytes. The impact of mim222 seen on *Cd36* agrees with data obtained in rats with metabolic syndrome features, which have compromised *Cd36* expression in adipocytes and the hyperlipidemia related

phenotype is ameliorated in transgenic mice overexpressing this gene.⁴⁶ Moreover, in humans, a genetic deficiency of this gene is associated with IR and hyperlipidemia.⁴⁷ Therefore, the reduction observed in *Cd36* associated with mim222 would be related to a disturbed lipid metabolism and linked to the malfunction of insulin signaling pathway. Concerning the impact on *Lpl*, fat-specific *Lpl* KO mice models do not show variations in body weight or body composition.⁴⁸ Therefore, a direct relationship between its repression and obese phenotype has not been discerned. Nonetheless, *Lpl* expression in adipose tissue is positively regulated posttranscriptionally and posttranslationally by insulin.⁴⁹ Thus, the impairment observed in insulin signaling pathway could be direct or indirectly responsible of this downregulation, rather than a direct effect of mim222.

Finally, signaling pathways involving PPAR γ were also found repressed in transcriptomic analysis in both stages and this was confirmed at the individual gene level in preadipocytes. PPAR γ is the major regulator of adipogenesis, the cell differentiation process from preadipocytes to mature adipocytes. Its reduction has been shown to impair the normal properties of mature 3T3-L1 adipocytes limiting cell size expansion, fatty acid uptake and glucose transport while increasing the rate of lipolysis.⁵⁰ Interestingly, this metabolic profile is achieved through downregulation of key genes such as *Slc2a4*, *Insr*, and *Irs1*,⁵⁰ which is in accordance with the effects promoted by mim222 in our cell system. In addition, other studies demonstrate that adipo-specific KO of *Ppar γ* in mice leads to IR, adipocyte hypocellularity and hypertrophy and dysregulated lipid metabolism.⁵¹ However, the expected reduction of lipid accumulation and/or change on cells morphology could not be observed in mature adipocytes. That is probably because PPAR γ is acting in concerted action with other related signals at a multi-tissue level, which could not be appreciated in the cell culture system. Nonetheless, a link between *Ppar γ* downregulation mediated by miR-222 and an impairment of adipocyte function that might contribute to the onset of metabolic syndrome cannot be discarded.

The significant global effect of mim222 treatment at transcriptional level in preadipocytes was maintained, although diluted, after cell differentiation, as mature adipocytes showed some signaling routes altered but a normalized expression in most of individual genes studied. Despite this reversion in gene expression, at the translational level the impact was seen exclusively on mature adipocytes, strengthening the idea that mim222 treatment had consequences even after cell specialization. It is noteworthy this delayed response of mim222 treatment on protein levels compared to mRNAs levels. miRNAs can act through mRNA decay or translation inhibition.⁵² In mammalian cells, the former repression effect is

predominant and begins after approximately 6 h of miRNA induction.⁵² This could explain the fact that mRNA levels were importantly diminished in preadipocytes, after 48 h of exposure to mim222, while protein levels remained unaltered in this cell stage. Moreover, “large oscillations in protein levels in response to an oscillating miRNA require a fast protein turnover rate.”⁵³ This is not the case for the proteins that were significantly repressed in mature adipocytes: PTEN has an average protein half-life of 132.5 h, while AKT presents 41.1 h (measured in mouse NIH 3T3 fibroblasts⁵⁴). Therefore, it could be suggested that during cell differentiation (from day 2 to 8), the slow cell turnover of these proteins could exacerbate the repression of mim222 on translation; while the more rapid turnover of the respective mRNA (11.9 h for PTEN and 13.6 h for AKT⁵⁴) normalized the transcriptional impact. In addition, the late response in the protein levels could also be related to a cell memory effect, promoting the acquisition of memories by the early transfection of mim222, which would lead to phenotypic adaptations in subsequent challenges. The long-lasting effect promoted by mim222 could be driven by epigenetic mechanisms as, in fact, miRNAs can exert changes in the methylation of certain genes.⁵⁵ Thus, changes triggered by miR-222 in the gene expression of adipocytes herein outlined might cause relevant cell imprinting during crucial periods of the developmental programming and have future implications, even when the transcriptional impact on particular genes was partially reversed.

In conclusion, these results have contributed to the elucidation of the molecular mechanisms involved in the action of this miRNA and to dissect its specific effects on adipocytes. Altogether, exogenous induced miR-222 in the 3T3-L1 cell line exerted targeted impact in crucial routes for adipocyte programming and function and, in particular, on insulin-related signaling pathways. The modulation was mainly observed through negative transcriptional regulation of main signaling routes and accompanied by the activation of potential compensatory pathways. These outcomes are in agreement with previous studies in which miR-222 has been associated with metabolic syndrome and, in particular, with IR in animal models.^{5–9} In addition, the role of miR-222 in metabolic programming was also suggested and fits with data from *in vivo* studies carried by our group.^{13,19} It is plausible to suggest that miR-222 impact on gene expression could be in part responsible of this thin-outside-fat-inside phenotype, as a long-lasting effect of the early treatment was implemented at some extent. Nonetheless, in the *in vivo* approach, rats are exposed to significant levels of miR-222 through breast milk, thus receiving multiple physiological doses during a longer period, in contrast to the acute high dose that was herein applied. Consequently,

this work strengthens the potential role that miR-222 plays in metabolic programming and further research should be conducted to elucidate its concrete impact *in vivo*.

AUTHOR CONTRIBUTIONS

Pere Bibiloni and Catalina A. Pomar performed research. Francisca Serra, Joana Sánchez, and Catalina A. Pomar designed research. Pere Bibiloni, Catalina A. Pomar, Francisca Serra, and Joana Sánchez analyzed data. Pere Bibiloni, Catalina A. Pomar, and Juana Sánchez wrote the first draft of the manuscript. All the authors worked on the revisions and final version of the paper. All authors have revised the manuscript and approved the final version.

ACKNOWLEDGMENTS

This research was supported by Project “PI20/00417”, funded by Instituto de Salud Carlos III and “Fondo Europeo de Desarrollo Regional Una Manera de hacer Europa”. The Research Group Nutrigenomics, Biomarkers and Risk Evaluation receives financial support from Instituto de Salud Carlos III and Centro de Investigación Biomédica en Red Fisiopatología de la Obesidad y Nutrición (CIBERObn). PB has a predoctoral research contract (FPU20/06023 - Ministerio de Universidades).

FUNDING INFORMATION

This research was supported by the project “PI17/01614”, funded by Instituto de Salud Carlos III and co-funded by European Union (ERDF/ESF, “Investing in your future”).

CONFLICT OF INTEREST


The authors declare that they have no conflict of interest.

DATA AVAILABILITY STATEMENT

Data available in article supplementary material. Additional data available on request from the authors.

ORCID

Pere Bibiloni  <https://orcid.org/0000-0002-3980-0270>

Catalina A. Pomar  <https://orcid.org/0000-0002-8113-761X>

Andreu Palou  <https://orcid.org/0000-0002-0295-4452>

Juana Sánchez  <https://orcid.org/0000-0002-9176-8060>

Francisca Serra  <https://orcid.org/0000-0002-8307-9732>

REFERENCES

1. Bartel DP. Metazoan MicroRNAs. *Cell*. 2018;173:20–51.
2. Wang Y, Liang Y, Lu Q. MicroRNA epigenetic alterations: predicting biomarkers and therapeutic targets in human diseases. *Clin Genet*. 2008;74:307–15.



3. Li Y, Kowdley KV. MicroRNAs in common human diseases. *Genom Proteom Bioinform*. 2012;10:246–53.
4. Deiuliis JA. MicroRNAs as regulators of metabolic disease: pathophysiologic significance and emerging role as biomarkers and therapeutics. *Int J Obes (Lond)*. 2016;40:88–101.
5. Ortega FJ, Mercader JM, Catalán V, Moreno-Navarrete JM, Pueyo N, Sabater M, et al. Targeting the circulating microRNA signature of obesity. *Clin Chem*. 2013;59:781–92.
6. Chartoumpakis DV, Zaravinos A, Ziros PG, Iskrenova RP, Psyrogiannis AI, Kyriazopoulou VE, et al. Differential expression of microRNAs in adipose tissue after long-term high-fat diet-induced obesity in mice. *PLoS One*. 2012;7:34872.
7. Herrera BM, Lockstone HE, Taylor JM, Ria M, Barrett A, Collins S, et al. Global microRNA expression profiles in insulin target tissues in a spontaneous rat model of type 2 diabetes. *Diabetologia*. 2010;53:1099–109.
8. Cui X, You L, Zhu L, Wang X, Zhou Y, Li Y, et al. Change in circulating microRNA profile of obese children indicates future risk of adult diabetes. *Metabolism*. 2018;78:95–105.
9. Ortega FJ, Mercader JM, Moreno-Navarrete JM, Rovira O, Guerra E, Esteve E, et al. Profiling of circulating microRNAs reveals common microRNAs linked to type 2 diabetes that change with insulin sensitization. *Diabetes Care*. 2014;37:1375–83.
10. Weber JA, Baxter DH, Zhang S, Huang DY, Huang KH, et al. The microRNA spectrum in 12 body fluids. *Clin Chem*. 2010;56:1733–41.
11. Xi Y, Jiang X, Li R, Chen M, Song W, Li X. The levels of human milk microRNAs and their association with maternal weight characteristics. *Eur J Clin Nutr*. 2016;70:445–9.
12. Zamanillo R, Sánchez J, Serra F, Palou A. Breast milk supply of microRNA associated with leptin and adiponectin is affected by maternal overweight/obesity and influences infancy BMI. *Nutrients*. 2019;11:2589.
13. Pomar CA, Castro H, Picó C, Serra F, Palou A, Sánchez J. Cafeteria diet consumption during lactation in rats, rather than obesity per se, alters miR-222, miR-200a, and miR-26a levels in milk. *Mol Nutr Food Res*. 2019;63:1800928.
14. Munch EM, Harris RA, Mohammad M, Benham AL, Pejerrey SM, Showalter L, et al. Transcriptome profiling of microRNA by next-gen deep sequencing reveals known and novel miRNA species in the lipid fraction of human breast Milk. *PLoS One*. 2013;8:e50564.
15. Reynolds CM, Gray C, Li M, Segovia SA, Vickers MH. Early life nutrition and energy balance disorders in offspring in later life. *Nutrients*. 2015;7:8090–111.
16. Langley-Evans SC. Nutrition in early life and the programming of adult disease: a review. *J Hum Nutr Diet*. 2015;28:1–14.
17. Melnik BC, John SM, Schmitz G. Milk: an exosomal microRNA transmitter promoting thymic regulatory T cell maturation preventing the development of atopy? *J Transl Med*. 2014;12:43.
18. Zhou Q, Li M, Wang X, Li Q, Wang T, Zhu Q, et al. Immune-related microRNAs are abundant in breast milk exosomes. *Int J Biol Sci*. 2011;8:118–23.
19. Pomar CA, van Nes R, Sánchez J, Picó C, Keijer J, Palou A. Maternal consumption of a cafeteria diet during lactation in rats leads the offspring to a thin-outside-fat-inside phenotype. *Int J Obes (Lond)*. 2017;41:1279–87.
20. Pomar CA, Castro H, Picó C, Palou A, Sánchez J. Maternal overfeeding during lactation impairs the metabolic response to fed/fasting changing conditions in the postweaning offspring. *Mol Nutr Food Res*. 2019;63:1900504.
21. Pomar CA, Picó C, Palou A, Sánchez J. Maternal consumption of a cafeteria diet during lactation leads to altered diet-induced thermogenesis in descendants after exposure to a Western diet in adulthood. *Nutrients*. 2022;14:1958.
22. Pomar CA, Serra F, Palou A, Sánchez J. Lower miR-26a levels in breastmilk affect gene expression in adipose tissue of offspring. *FASEB J*. 2021;35:e21924.
23. Hidalgo MR, Cubuk C, Amadoz A, Salavert F, Carbonell-Caballero J, Dopazo J. High throughput estimation of functional cell activities reveals disease mechanisms and predicts relevant clinical outcomes. *Oncotarget*. 2017;8:5160–78.
24. Yang YF, Wang F, Xiao JJ, Song Y, Zhao YY, Cao Y, et al. MiR-222 overexpression promotes proliferation of human hepatocellular carcinoma HepG2 cells by downregulating p27. *Int J Clin Exp Med*. 2014;7:893–902.
25. Chen Y, Wang X. MiRDB: an online database for prediction of functional microRNA targets. *Nucleic Acids Res*. 2020;48:D127–31.
26. Qi R, Han X, Wang J, Qiu X, Wang Q, Yang F. MicroRNA-489-3p promotes adipogenesis by targeting the Postn gene in 3T3-L1 preadipocytes. *Life Sci*. 2021;278:119620.
27. Nunes ADC, Weigl M, Schneider A, Nouredine S, Yu L, Lahde C, et al. miR-146a-5p modulates cellular senescence and apoptosis in visceral adipose tissue of long-lived Ames dwarf mice and in cultured pre-adipocytes. *GeroScience*. 2022;44:503–18.
28. Xie H, Lim B, Lodish HF. MicroRNAs induced during adipogenesis that accelerate fat cell development are downregulated in obesity. *Diabetes*. 2009;58:1050–7.
29. Softic S, Boucher J, Solheim MH, Fujisaka S, Haering MF, Homan EP, et al. Lipodystrophy due to adipose tissue-specific insulin receptor knockout results in progressive NAFLD. *Diabetes*. 2016;65:2187–200.
30. Sasaki T, Kuroko M, Sekine S, Matsui S, Kikuchi O, Susanti VY, et al. Overexpression of insulin receptor partially improves obese and diabetic phenotypes in db/db mice. *Endocr J*. 2015;62:787–96.
31. Tang CY, Man XF, Guo Y, Tang HN, Tang J, Zhou CL, et al. IRS-2 partially compensates for the insulin signal defects in IRS-1^{-/-} mice mediated by miR-33. *Mol Cells*. 2017;40:123–32.
32. Ono K, Igata M, Kondo T, Kitano S, Takaki Y, Hanatani S, et al. Identification of microRNA that represses IRS-1 expression in liver. *PLoS One*. 2018;13:e0191553.
33. Winnay JN, Solheim MH, Dirice E, Sakaguchi M, Noh HL, Kang HJ, et al. PI3-kinase mutation linked to insulin and growth factor resistance in vivo. *J Clin Invest*. 2016;126:1401–12.
34. Huang-Doran I, Tomlinson P, Payne F, Gast A, Sleigh A, et al. Insulin resistance uncoupled from dyslipidemia due to C-terminal PIK3R1 mutations. *JCI Insight*. 2016;1:e88766.
35. Rancourt RC, Ott R, Schellong K, Melchior K, Ziska T, Henrich W, et al. Visceral adipose tissue alteration of PI3KR1 expression is associated with gestational diabetes but not promoter DNA methylation. *Adipocyte*. 2019;8:339–46.
36. Zhang Z, Liu H, Liu J. Akt activation: a potential strategy to ameliorate insulin resistance. *Diabetes Res Clin Pract*. 2019;156:107092.

37. Lu M, Wan M, Leavens KF, Chu Q, Monks BR, Fernandez S, et al. Insulin regulates liver metabolism in vivo in the absence of hepatic Akt and Foxo1. *Nat Med.* 2012;18:388–95.
38. Kurlawalla-Martinez C, Stiles B, Wang Y, Devaskar SU, Kahn BB, Wu H. Insulin hypersensitivity and resistance to streptozotocin-induced diabetes in mice lacking PTEN in adipose tissue. *Mol Cell Biol.* 2005;25:2498–510.
39. Ruderman NB, Carling D, Prentki M, Cacicedo JM. AMPK, insulin resistance, and the metabolic syndrome. *J Clin Investig.* 2013;123:2764–72.
40. Chadt A, Al-Hasani H. Glucose transporters in adipose tissue, liver, and skeletal muscle in metabolic health and disease. *Pflügers Arch.* 2020;472:1273–98.
41. Yang Q, Graham TE, Mody N, Preitner F, Peroni OD, Zabolotny JM, et al. Serum retinol binding protein 4 contributes to insulin resistance in obesity and type 2 diabetes. *Nature.* 2005;436:356–62.
42. Stenbit AE, Tsao TS, Li J, Burcelin R, Geenen DL, Factor SM, et al. GLUT4 heterozygous knockout mice develop muscle insulin resistance and diabetes. *Nat Med.* 1997;3:1096–101.
43. Shepherd PR, Kahn BB. Glucose transporters and insulin action—implications for insulin resistance and diabetes mellitus. *New Engl J Med.* 1999;341:248–57.
44. Yang T, Espenshade PJ, Wright ME, Yabe D, Gong Y, Aebersold R, et al. Crucial step in cholesterol homeostasis: sterols promote binding of SCAP to INSIG-1, a membrane protein that facilitates retention of SREBPs in ER. *Cell.* 2002;110:489–500.
45. Carobbio S, Hagen RM, Lelliott CJ, Slawik M, Medina-Gomez G, Tan CY, et al. Adaptive changes of the Insig1/SREBP1/SCD1 set point help adipose tissue to cope with increased storage demands of obesity. *Diabetes.* 2013;62:3697–708.
46. Aitman TJ, Glazier AM, Wallace CA, Cooper LD, Norsworthy PJ, Wahid FN, et al. Identification of Cd36 (fat) as an insulin-resistance gene causing defective fatty acid and glucose metabolism in hypertensive rats. *Nat Genet.* 1999;21:76–83.
47. Kuwasako T, Hirano KI, Sakai N, Ishigami M, Hiraoka H, Yakub MJ, et al. Lipoprotein abnormalities in human genetic CD36 deficiency associated with insulin resistance and abnormal fatty acid metabolism. *Diabetes Care.* 2003;26:1647–8.
48. Weinstock PH, Levak-Frank S, Hudgins LC, Radner H, Friedman JM, Zechner R, et al. Lipoprotein lipase controls fatty acid entry into adipose tissue, but fat mass is preserved by endogenous synthesis in mice deficient in adipose tissue lipoprotein lipase. *Proc Natl Acad Sci U S A.* 1997;94:10261–6.
49. Semenkovich CF, Wims M, Noe L, Etienne J, Chan L. Insulin regulation of lipoprotein lipase activity in 3T3-L1 adipocytes is mediated at posttranscriptional and posttranslational levels. *J Biol Chem.* 1989;264:9030–8.
50. Tamori Y, Masugi J, Nishino N, Kasuga M. Role of peroxisome proliferator-activated receptor- γ in maintenance of the characteristics of mature 3T3-L1 adipocytes. *Diabetes.* 2002;51:2045–55.
51. He W, Barak Y, Hevener A, Olson P, Liao D, le J, et al. Adipose-specific peroxisome proliferator-activated receptor γ knockout causes insulin resistance in fat and liver but not in muscle. *Proc Natl Acad Sci U S A.* 2003;100:15712–7.
52. Eichhorn SW, Guo H, McGeary SE, Rodriguez-Mias RA, Shin C, Baek D, et al. mRNA destabilization is the dominant effect of mammalian microRNAs by the time substantial repression ensues. *Mol Cell.* 2014;56:104–15.
53. Hausser J, Syed AP, Selevsek N, Van Nimwegen E, Jaskiewicz L, et al. Timescales and bottlenecks in miRNA-dependent gene regulation. *Mol Syst Biol.* 2013;9:711.
54. Schwanhüusser B, Busse D, Li N, Dittmar G, Schuchhardt J, et al. Global quantification of mammalian gene expression control. *Nature.* 2011;473:337–42.
55. Fuso A, Raia T, Orticello M, Lucarelli M. The complex interplay between DNA methylation and miRNAs in gene expression regulation. *Biochimie.* 2020;173:12–6.

SUPPORTING INFORMATION

Additional supporting information can be found online in the Supporting Information section at the end of this article.

How to cite this article: Bibiloni P, Pomar CA, Palou A, Sánchez J, Serra F. miR-222 exerts negative regulation on insulin signaling pathway in 3T3-L1 adipocytes. *BioFactors.* 2022. <https://doi.org/10.1002/biof.1914>